



AFRL-AFOSR-JP-TR-2016-0061

Multi-Ferroic Polymer Nanoparticle Composites for Next
Generation Metamaterials

Sylvie Begin-Colin
UNIVERSITE DE STRASBOURG
4 RUE BLAISE PASCAL
STRASBOURG, 67000
FR

06/15/2016
Final Report

DISTRIBUTION A: Distribution approved for public release.

Air Force Research Laboratory
Air Force Office of Scientific Research
Asian Office of Aerospace Research and Development
Unit 45002, APO AP 96338-5002

REPORT DOCUMENTATION PAGE				Form Approved OMB No. 0704-0188	
<p>The public reporting burden for this collection of information is estimated to average 1 hour per response, including the time for reviewing instructions, searching existing data sources, gathering and maintaining the data needed, and completing and reviewing the collection of information. Send comments regarding this burden estimate or any other aspect of this collection of information, including suggestions for reducing the burden, to Department of Defense, Executive Services, Directorate (0704-0188). Respondents should be aware that notwithstanding any other provision of law, no person shall be subject to any penalty for failing to comply with a collection of information if it does not display a currently valid OMB control number.</p> <p>PLEASE DO NOT RETURN YOUR FORM TO THE ABOVE ORGANIZATION.</p>					
1. REPORT DATE (DD-MM-YYYY) 15-06-2016		2. REPORT TYPE Final		3. DATES COVERED (From - To) 30 Sep 2012 to 29 Sep 2015	
4. TITLE AND SUBTITLE Multi-Ferroic Polymer Nanoparticle Composites for Next Generation Metamaterials				5a. CONTRACT NUMBER	
				5b. GRANT NUMBER FA2386-12-1-4014	
				5c. PROGRAM ELEMENT NUMBER 61102F	
6. AUTHOR(S) Sylvie Begin-Colin				5d. PROJECT NUMBER	
				5e. TASK NUMBER	
				5f. WORK UNIT NUMBER	
7. PERFORMING ORGANIZATION NAME(S) AND ADDRESS(ES) UNIVERSITE DE STRASBOURG 4 RUE BLAISE PASCAL STRASBOURG, 67000 FR				8. PERFORMING ORGANIZATION REPORT NUMBER	
9. SPONSORING/MONITORING AGENCY NAME(S) AND ADDRESS(ES) AOARD UNIT 45002 APO AP 96338-5002				10. SPONSOR/MONITOR'S ACRONYM(S) AFRL/AFOSR IOA	
				11. SPONSOR/MONITOR'S REPORT NUMBER(S) AFRL-AFOSR-JP-TR-2016-0061	
12. DISTRIBUTION/AVAILABILITY STATEMENT A DISTRIBUTION UNLIMITED: PB Public Release					
13. SUPPLEMENTARY NOTES					
14. ABSTRACT <p>The research investigates on design and characterizations of raspberry shaped nanostructures for flexible magnetodielectric composites. These structures improve the saturation magnetization substantially compared to conventional magnetic nanoparticles by their collective oriented organization in a single nanostructure. As a result, the structures can be used developing materials with high permeability (μ), permittivity (ϵ) and minimal dielectric and magnetic loss ($\tan \delta$). These materials are appealing for the development of microwave communications devices that can operate at higher than 1GHz.</p>					
15. SUBJECT TERMS <p>Magnetoresistance, Metamaterials, Nanocomposites, Nanoparticles</p>					
16. SECURITY CLASSIFICATION OF:			17. LIMITATION OF ABSTRACT SAR	18. NUMBER OF PAGES 14	19a. NAME OF RESPONSIBLE PERSON MAH, MISOON
a. REPORT Unclassified	b. ABSTRACT Unclassified	c. THIS PAGE Unclassified			19b. TELEPHONE NUMBER (Include area code) 042-511-2001

**Multi-Ferroic Polymer Nanoparticle Composites for Next Generation Metamaterials
AOARD 124014**

Final Report – S. Begin – IPCMS Strasbourg France

Researchers involved in this project :

Peter Kofinas, University of Maryland, USA, kofinas@umd.edu

Sylvie Begin-Colin, CNRS-UDS, France, sylvie.begin@unistra.fr

Yuanzhe Piao, Seoul National University, Korea, parkat9@snu.ac.kr

Introduction	1
Abstract : Design and characterizations of raspberry shaped nanostructures for flexible magnetodielectric composites	2
Report :	3
1. Synthesis mechanism of raspberry shaped nanostructures.	3
2. Design and structural and magnetic characterizations of citrated raspberry nanostructures for the fabrication of stretchable magneto-dielectric composites. .	7
Conclusions and Future Work	11

Introduction

The aim of this project was the development of magnetodielectric polymer composites consisting of magnetic nanoparticles that possess high permeability (μ), permittivity (ϵ) and minimal dielectric and magnetic loss ($\tan \delta$). Materials with high dielectric constant (ϵ) and permeability (μ) are appealing for the development of microwave communications devices. Polymer based composite materials that possess high ϵ and μ are receiving a lot of interest recently, due to their malleability, low weight, and elastic properties. It is important however to note that conventional ferrite-polymer composites are limited to operating frequencies much lower than 1 GHz since their μ values decay rapidly beyond their resonance frequency (f_{res}). The best known examples are MnZn and NiZn ferrites which exhibit a f_{res} of 2MHz and 200MHz, respectively. Ferrites, particularly magnetite, have low saturation magnetization (M_s) by comparison to metals, which limits the product of μ and f_{res} as estimated via the Snoek limit. Thus, it is extremely difficult to obtain composites with high μ values at high operational frequencies using ferrites nanoparticles. However it has been recently demonstrated that it is possible to enhance the limited magnetic properties of magnetite nanoparticles by synthesizing nanostructures consisting of oriented aggregates of ferrite nanocrystals. These nanostructures also termed *raspberry nanostructures* consist of nanocrystals with common crystallographic orientations directly combined together to form larger ones, which leads to magnetic collective assembly properties.

The french group of S. Begin has developed the synthesis and the structural and magnetic characterisations of these *raspberry nanostructures* in this AOARD project. Dr Yuanzhe Piao at Seoul National University, Seoul, Korea, has developed the synthesis of silica coated magnetite nanoparticles with regular magnetic properties. Professor Kofinas at the University of Maryland, College Park, MD, has developed the fabrication/characterization of flexible magnetodielectric composites using the aforementioned magnetite nano-objects.

Abstract : Design and characterizations of raspberry shaped nanostructures for flexible magnetodielectric composites

Traditional magnetite nanoparticles have a saturation magnetization between 45 emu/g and 55 emu/g due to surface and volume spin canting and defects. However, it has been recently demonstrated that it is possible to improve the saturation magnetization of magnetite nanoparticles by their collective oriented organization in a single nanostructure. The research group of Pr. Sylvie Begin-Colin at IPCMS has synthesized corona shaped magnetite nanostructures that acquire collective assembly during synthesis. These nanostructures displaying a “raspberry” morphology have been synthesized by a solvo-thermal method adapted from Cheng et al. [*J. Chen et al. Adv. Mater.* 17, (2005), 582-586]. Nanostructures consist of spherical aggregates of small nanocrystals that exhibit hollow structures. The nanostructure size may be tuned in the range of 100 - 500 nm, and the nanocrystal sizes are modulated between 2 nm and 30 nm. These different nanostructures obtained by varying the reaction conditions (reaction time, reactants concentration) have been carefully characterized by different techniques such as HR-TEM, 3D tomography, SEM, BET, TGA, XRD, etc. Furthermore, the different reaction steps occurring during the synthesis have been investigated more intensively by following the temperature and pressure evolutions inside an instrumented autoclave. To produce larger amount of raspberry shaped nanostructures (RSNs) necessary for magneto dielectric measurements, another bigger autoclave has been built and allowed producing 20h/batch. It has allowed providing the large amount of nanostructures to perform measurements at various frequencies. This synthesis part has led to a paper which should be submitted before June 2016, entitled “Formation Mechanism of Iron Oxide Raspberry Shaped Nanostructures” by Olivier Gerber, Benoit P. Pichon, Dris Ihwakrim, Ileana Florea, Simona Moldovan, Ovidiu Ersen, Dominique Begin, Jean-Marc Grenèche, Sebastien Lemonnier, Elodie Barraud, Sylvie Begin-Colin.

Two types of corona magnetite nanostructures with a mean size of 250 nm consisting of an orientated assembly of smaller magnetite nanoparticles with sizes either of 5 nm or 25 nm have been selected for the fabrication of flexible magnetodielectric composites by Professor Kofinas. First experiments have been performed with as synthesized RSNs by Pr Peter Kofinas but the dispersion of RSNs in the polymer matrix was not optimal. Therefore other batches of RSNs have been synthesized and citrated before sending them to Pr Kofinas. These citrated nanostructures, which are monocrystalline due to an oriented aggregation induced by the synthesis process, have achieved saturation magnetization values of 74 emu/g and 88 emu/g, respectively. Another important magnetic aspect of such RSNs is their infinitesimally small coercivity. Such magnetic nanostructures with high saturation magnetization and low levels of coercivity were shown to be promising candidates for magnetic fillers to fabricate high performance flexible magnetodielectric composites. This part has led to a published paper in *J. Mater. Chem. C*, 2016,4, 2345 entitled “Stretchable Magneto-dielectric Composites Based on Raspberry-Shaped Iron Oxide Nanostructures” by Mert Vural, Olivier Gerber, Benoit P. Pichon, Sebastien Lemonnier, Elodie Barraud, Leo C. Kempel, Sylvie Begin-Colin and Peter Kofinas.

Report :

1. Synthesis mechanism of raspberry shaped nanostructures.

Iron oxide porous nanostructures have been synthesized by a modified polyol solvothermal approach involving iron chloride hexahydrate, urea, ethylenglycol and succinic acid as reactants. When the reaction is performed for 13 h under solvothermal conditions in a Teflon lined autoclave at 200 °C, a black powder is obtained which is washed successively with water and ethanol. SEM micrograph showed particles featured by a spherical shape and a size distribution centered to 250 nm (Figure 1a). They consist in aggregates of nanograins of 25 nm as shown by TEM micrographs (Figure 1b). Nanostructures are mainly constituted in the magnetite phase ($a = 8.39(7)$ Å to compare to that of stoichiometric magnetite $a = 8.396$ Å (magnetite JCPDS file 19-629) and 70% of magnetite from Mössbauer spectra) (Figure 1f) and are featured by similar crystal orientation. Their saturation magnetisation is about 81 emu/g, larger than that of individual 25 nm sized iron oxide NPs. Furthermore, SEM micrographs showed some cavity of about 90 nm in broken RSNs which corresponds to a hollow structure (Figure 1d). It was confirmed by studying the cross-section of these objects after their embedding in a resin followed by a polishing step (Figure 1e).

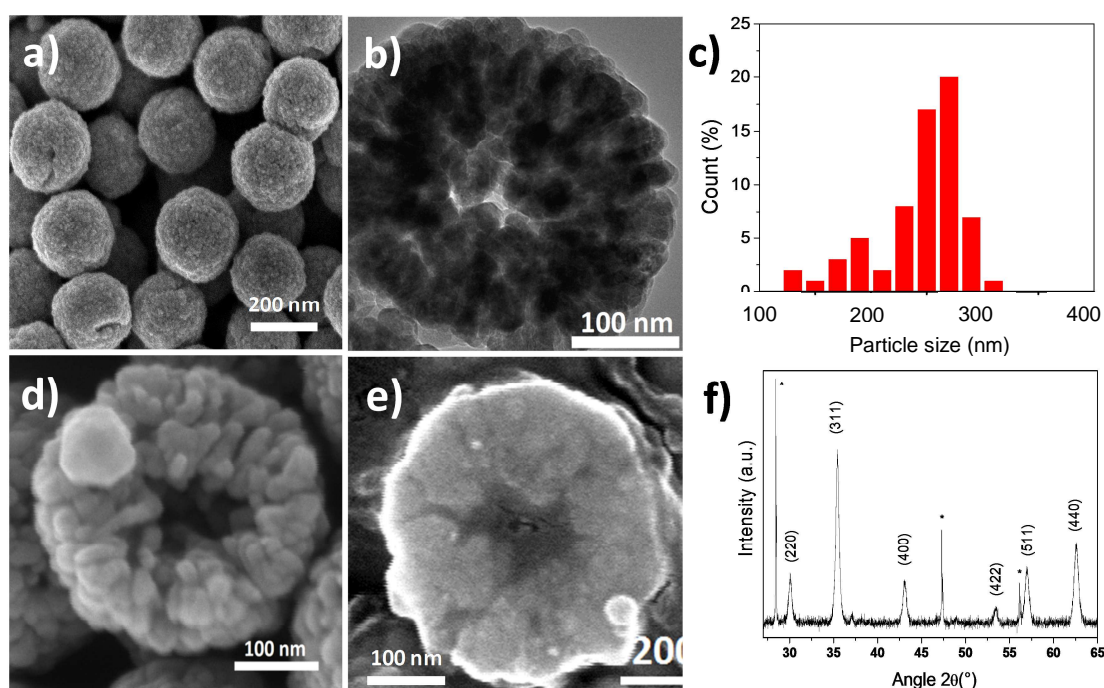


Figure 1. RSNs obtained after 13 h of reaction. a) SEM micrograph. b) TEM micrograph. c) Size distribution. SEM images on d) broken RSN and e) on the cross-section after embedding in a resin matrix and polishing. f) XRD pattern, stars correspond to silicon which used as a reference.

For a better understanding of the reaction mechanism, a time-resolved study has been performed by SEM on samples collected after different reaction times (Figure 2 and schema 1). After 4 hours of reaction, a gel-like structure with non-regular shape grains has been observed (Figure 2a), which is amorphous according to XRD analysis (not shown). FTIR spectrum exhibits $\nu\text{Fe-O}$ and $\nu\text{C-H}$ bands at 500 cm^{-1} and 2900 cm^{-1} , respectively which suggests the formation of

an iron oxide based complex. After 5 h, the amorphous compound is no longer present and rather plate-like structures (PLS) with irregular morphologies (Figure 2b) and some small RSNs (with a mean size of about 100 nm) were observed (Figure S3 mais qui devient S2). After 6 h, RSNs are exclusively observed and are featured by a rather large bimodal size distribution with two main sizes centered to 90 nm and 200 nm with a heterogeneous nanograin (NG) size around 3-5 nm (Figure 2c). The mean RSN size get quite homogeneous after 7 h with a mean size of 250 nm with dispersion from 50 to 70 nm and then does not increase with reaction time. In contrast, the NG size increases gradually with the reaction time (up to 13 h). The porous structure has been also investigated by performing nitrogen absorption-desorption measurements (Table 1). Specific surface areas were estimated by the Brunauer-Emmett-Teller model and decrease gradually when reaction time increases which is in agreement with the increase in the NG sizes. After 9 hours of reaction, the formation of a cavity is observed. The increase of grain size may be correlated to the formation of cavities in RSNs since, given the experimental conditions, longer reaction times favor inside-out (or inverse) Ostwald ripening. The inner part of RSNs solubilizes and recrystallizes onto grains located at the surface of RSNs. The observed synthesis pathway is described in Schema 1. To better understand the synthesis mechanisms, the PLS have been deeply investigated.

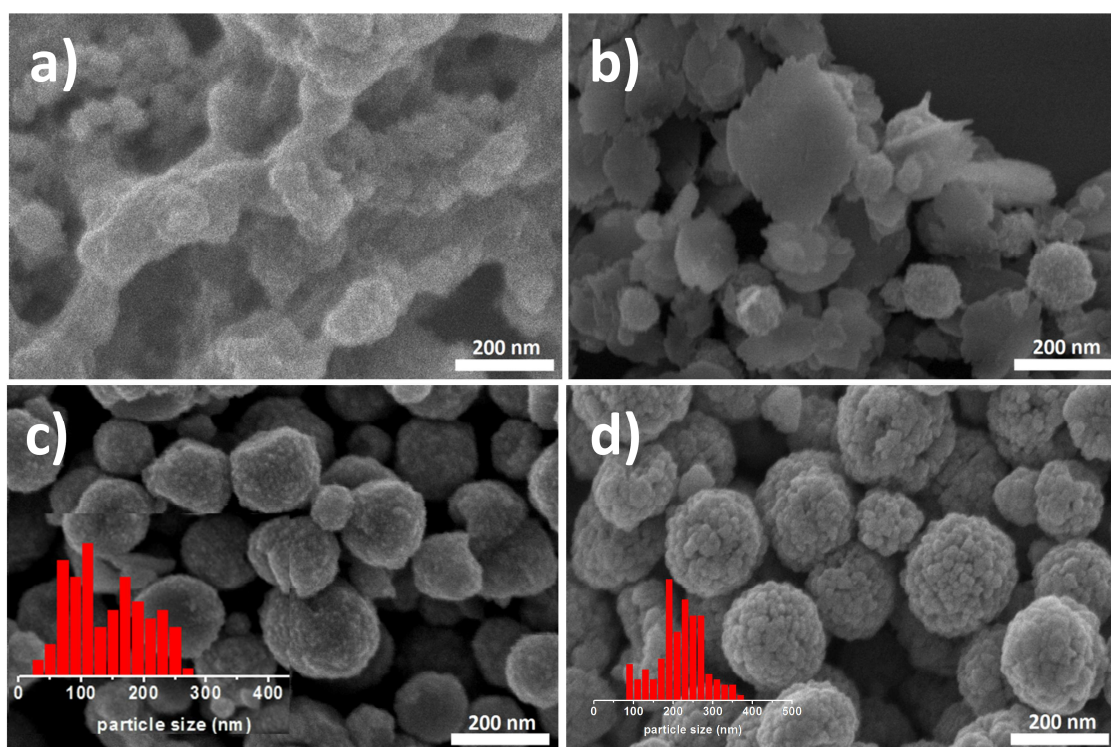


Figure 2. SEM micrographs corresponding to samples collected after a) 4 h, b) 5 h, c) 6 h and d) 9 h of reaction. Insets correspond to the size distribution measured from SEM micrographs.

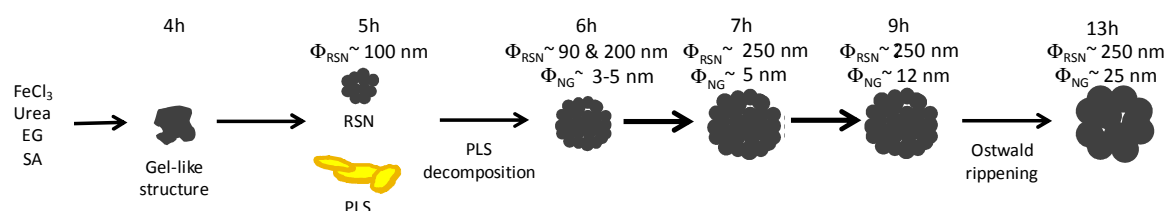
Table 1. Structural characteristics of raspberry-shaped nanostructures.

Reaction time	RSN size (nm)	Nanograin size (nm)	Surface specific area (m ² /g)
6h	90 & 200 ± 10	5 ± 3	61
7h	250 ± 50	5 ± 2	57
9h	250 ± 30	12 ± 2	38
12h	250 ± 12	25 ± 3	27

The intermediate formation of PLS is rather surprising and, to the best of our knowledge, has not been reported yet as an intermediate compounds in the synthesis of iron oxide nanocrystal clusters by the polyol solvothermal method. As they appear as key step in the synthesis process, their structure has been deeply investigated by TEM, TGA, IR and in situ TEM studies in temperature. This study is detailed in the paper to be submitted.

Discussion - reaction mechanism

The formation of RSNs is rather complex since the reaction proceeds through a multistep process (Scheme 1). The observation of the RSN synthesis at different reaction times has shown that an amorphous phase is formed after 4 hours and after 5 hours, small RSNs are observed together with PLS. When the reaction time increases, the PLS disappear simultaneously with the observation of a growth in the mean size of RSN (the NG size staying similar) which stabilizes after 7h of reaction. From 7h of reaction, the increase in the reaction time does not modify the mean size of RSNs while the mean size of NG increases and a core cavity forms.

Scheme 1. Schematic representation of the synthesis pathway.

The temperature and pressure have been recorded during the synthesis (Figure 3) in order to get a better understanding on the reaction mechanism. One may first notice that after 4h hours of reaction, the temperature and pressure are stabilized and the observed phases are thus formed in similar conditions of pressure and temperatures. An increase of pressure is observed after 2,5 h and is directly correlated to the endothermic peak at 130 °C in the temperature curve. These features correspond to the decomposition of urea in ammoniac which is catalyzed by hexahydrate Fe(III) chlorides. Indeed they are not observed when heating the reaction medium without using FeCl₃.6H₂O (Figure 3). Then ammonia reacts with water molecules leading to the formation of OH⁻ + NH₄⁺. These conditions (increases the alkalinity of the reaction media and presence of hydroxides) are well known to favor the co-precipitation of iron oxide NGs from intermediate iron hydroxides. That would explain the observation of small RSNs after 5 h of reaction.

However an amorphous phase is observed before at 4h and may be due to competitive interactions. Indeed when urea decomposes in ammoniac, alkaline conditions favor also the deprotonation of ethylene glycol which coordinate with Fe species. Therefore one may suggest that the amorphous phase observed after 4 h of reaction results from the competitive interaction of ammonia with water and EG leading thus to amorphous intermediate alkoxide and iron hydroxyde phases.

After 4 hours, the temperature and pressure reach their maximum and favor the formation of plate-like structures resulting from interaction of iron cations with OH⁻ and deprotonated ethylene glycol and the coprecipitation of small iron oxide NGs. The reaction conditions favor the aggregation of these NGs in nanostructures. The thermal studies performed on PLS have shown that these PLS are thermally stable at high temperature which explains that they are identified and also may be easily extracted from the reaction media after 4 h of reaction. Besides some PLS may be shown to be incorporated in RSNs. However at 4 h, the maximum temperature and pressure are reached and the PLS begin to decompose. PLS acts as an intermediate iron precursor (or iron reservoir) which decomposes at higher temperature and should induce heterogeneous nucleation of nanocrystals on previously formed iron oxide based RSNs. This would explain the increase of the mean RSNs size when that of NGs stays quite constant between 4 and 7 hours of reaction.

Such heterogeneous nucleation should favor the oriented aggregation of NGs which is emphasized by the high pressure and temperature conditions which lead to well-shaped RSNs with narrow size distribution after 7 h of reaction. From 7h, there are no more iron precursors available in the media and RSNs reach their maximum sizes. As the reaction time increases in these high pressure and temperature conditions, digestive inside-out Ostwald ripening proceeds to solubilization-recrystallization of grains. Nanograins located at the center of RSNs undergo solubilization while the ones located close to the surface grow with the reaction time.

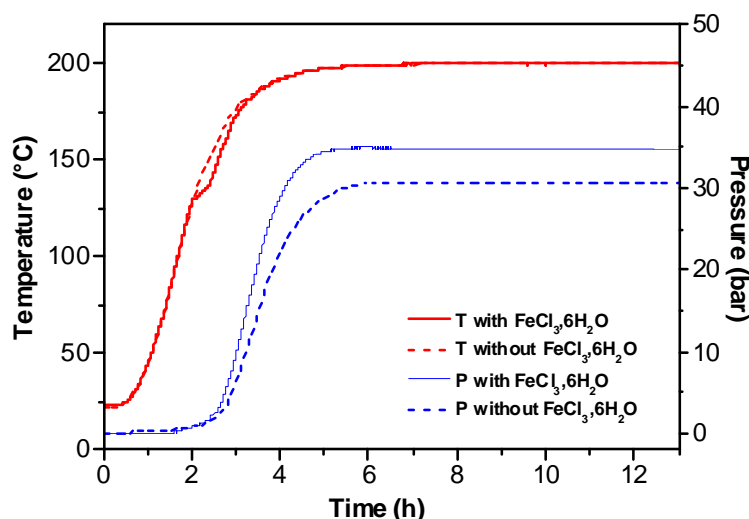


Figure 3. Temperature and pressure measurements as function of reaction time with (solid line) and without (dot line) iron chloride precursor.

Conclusion : The mechanism formation of porous raspberry shaped nanostructures synthesized by a one-pot polyol solvothermal method has been investigated in details from the early stages by using a combination of a wide panel of characterization techniques, namely SEM, TEM, XRD, FTIR spectroscopy, Mössbauer spectroscopy, elemental analysis, EELS and thermogravimetric analysis. A time resolved study demonstrates the intermediate formation of an amorphous iron alkoxide phase with a plate-like lamellar (PLS) structure. We showed thus that the synthesis of RSNs involved two iron precursors : the starting one and this in-situ formed iron alkoxide precursor which decomposes with time and heating and contributes to the growth step of nanostructures. Finally, a formation mechanism of RSN from such an original PLS structure, which is commonly admitted to proceed through the oriented aggregation of nanocrystals, has been proposed. Such a study will allow to propose strategies to dope these RSNs with other elements such as Mn, Co, Ni or Zn to improve their magnetic properties.

2. Design and structural and magnetic characterizations of citrated raspberry nanostructures for the fabrication of stretchable magneto-dielectric composites.

The iron oxide RSNs have been synthesized by a one-pot modified polyol solvothermal method. The reaction time may be used to alter the structure, composition and magnetic properties of the filler iron oxide RSNs (see § above). The solvothermal syntheses with reaction periods of 7 and 13 hours, result in spherical hollow clusters with a similar mean size around 250 nm and constituted of iron oxide nanocrystals with a mean nanocrystal size of 5 and 25 nm, respectively. These two types of RSNs have been selected for the fabrication of stretchable magneto-dielectric composites. However to favor their dispersion in polymer matrix, these RSNs have been citrated and their characterization is detailed below.

The structure of the RSNs fillers prepared using two reaction durations was characterized with X-Ray diffraction, Mössbauer spectroscopy and electron microscopies. The scanning electron microscopy (SEM) images revealed that both RSN fillers have an average diameter of about 250 nm (Figure 4 a, d). The surface roughness apparent in SEM images is indicative of a cluster-like structure. The transmission electron microscopy (TEM) characterization has demonstrated that these nanoclusters possess a hollow core, which validates the raspberry-like shape of this filler material (Figure 4a-inset, d, e). High-resolution TEM (HRTEM) images of the interface between two crystals in these RSN filler materials (Figure 5) and selected area electron diffraction (SAED) patterns (Figure 4c, f) confirm the oriented attachment of nanocrystals in RSNs. Indeed the HRTEM images clearly demonstrate that crystallographic orientations of nanocrystals are matched at the interface, which is indicative of a common crystal orientation shared by nanocrystals forming the RSN fillers (Figure 5). SAED patterns verified the formation of the spinel phase (Figure 4 c, e) and are consistent with single crystal structures (SAED patterns on single RSNs show Von Laue patterns instead of Debye rings). These observations show that RSNs are constituted of aggregated nanocrystals, which have similar crystallographic orientations.

The detailed characterization of the RSNs microstructure has showed that RSN fillers allowed to react for 7 hours (RSN5) have finer nanocrystal size than fillers allowed to react for 13 hours (RSN25) (Figure 4). From TEM micrographs, a mean nanocrystal size of 5 and 25 nm is determined for RSN5 and RSN25 respectively while crystallite sizes calculated from Rietveld analysis of X-Ray Diffraction (XRD) patterns (Figure 5b) are respectively 14 ± 1 and 15 ± 1 nm.

Such discrepancies between both measurements were related to the monocrystalline nature of the RSNs and the presence of defects or dislocation induced during the synthesis process. Indeed SAED patterns (Figure 4.c,f) and HRTEM of nanocrystal interfaces (Figure 5a) confirms the monocrystalline structure of RSNs, which is established with aggregates of nanocrystals with similar crystal orientations. However, the extended Von Laue spots in SAED patterns evidenced a slight misalignment in the orientation of these nanocrystals. In addition, Fast Fourier Transform (FFT) analysis performed on SAED patterns of RSNs has demonstrated the presence of defects.

XRD patterns of RSNs display characteristic peaks of the iron oxide spinel structure (Figure 5b). Lattice parameter deduced from XRD pattern is very close to that of stoichiometric magnetite for RSN25 and indicates an oxidized state for RSN5. In addition, Mössbauer spectroscopy confirmed that RSN fillers with smaller crystal size have a maghemite-rich composition ($\text{Fe}_{2.78}\text{O}_4$, 70% of maghemite) while those with large crystal size are mainly constituted of magnetite Fe_3O_4 phase ($\text{Fe}_{2.90}\text{O}_4$, 70% of magnetite). These variations in composition is explained by the surface oxidation of magnetite, which might be elevated due to smaller crystal size of maghemite-rich RSN fillers.

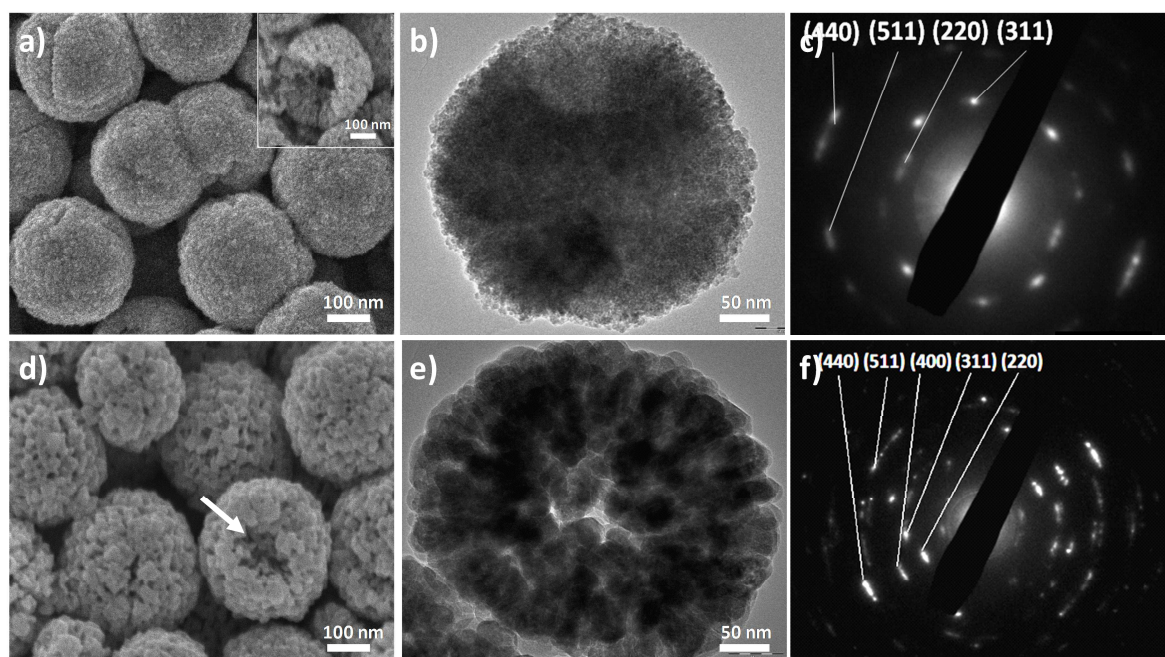


Figure 4. SEM images of citrate-capped RSNs reacted for (a) 7 hours, and (b) 13 hours. TEM images of citrate-capped RSNs reacted for (d) 7 hours, and (e) 13 hours. SAED patterns of citrate-capped RSNs reacted for (c) 7 hours, and (f) 13 hours.

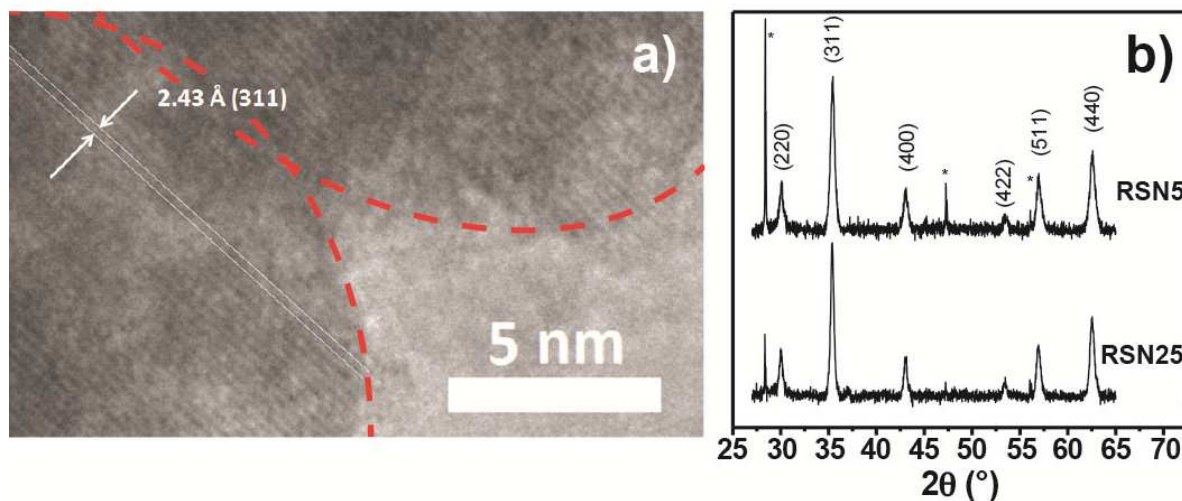


Figure 5. (a) HRTEM image of RSNs which shows on the nanostructure border that several nanocrystals display the same crystalline orientation. (b) XRD data for RSN5 and RSN25.

The characterization of the magnetic properties of RSN fillers correlates well with their structure and composition. The RSNs are superparamagnetic at 300K as the coercivity of both magnetite- and maghemite-rich RSNs at 5K remains below 300 Oe (Figure 6-insets), which is indicative of small nanocrystal size. The citrated RSN25 have demonstrated a M_s of 88 emu/g, which is comparable to the bulk M_s of magnetite (92 emu/g) and that of RSN5 is around 74 emu/g which is closed to bulk maghemite (Figure 6a,b). In contrast to RSNs, individual magnetite nanoparticles with a similar nanocrystal size have a saturation magnetization between 45 emu/g and 70 emu/g due to defects, surface and volume spin canting. In fact, the structuration of RSNs, which display aggregated orientation of nanocrystals has a critical role for improving the structural and magnetic order, limiting the influence of surface and volume spin canting. The strong dipolar interactions between nanocrystals forming RSNs favors the coupling of spins at the grain surface, which reduces the magnetic and structural disorder arising commonly from defects or broken bonds in the surface of iron oxide nanocrystals. Because of the strong dipolar interactions between nanocrystals, and the common crystallographic orientation of grains, RSNs exhibit higher crystal quality, and lower spin canting than individual iron oxide nanoparticles, which leads to magnetization values matching bulk materials.

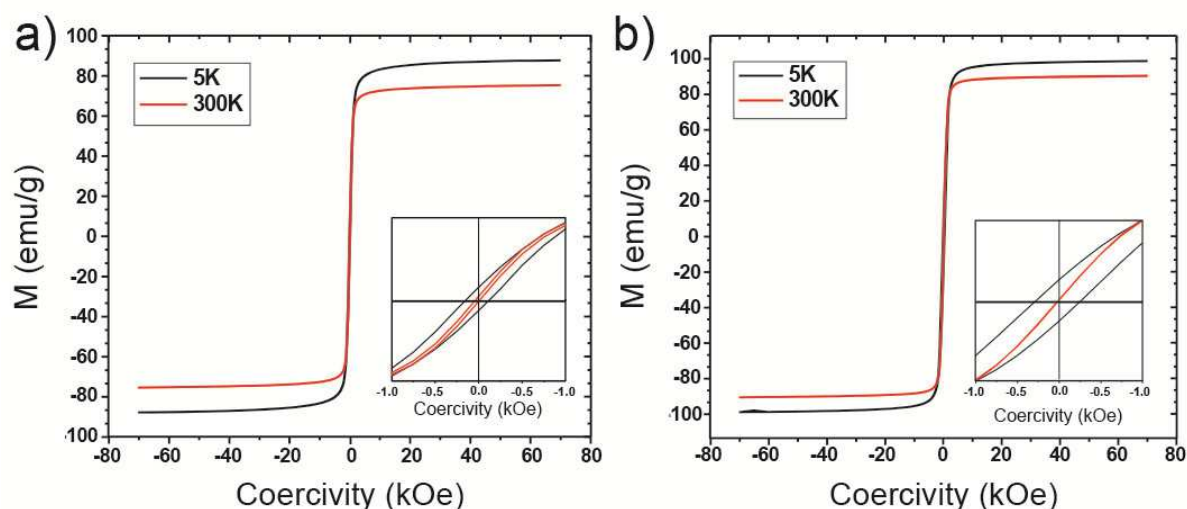


Figure 6. Magnetization curves for a) maghemite-rich (RSN5) and b) magnetite-rich (RSN25) RSNs at 5 K and 300K.

The influence of citrate capping on the surface charge of the RSNs was quantified using zeta potential experiments. The RSNs exhibited zeta potential values close to zero prior to attachment of the citrate capping agent, which is in agreement with the isoelectric point of iron oxide (IEP=6.8). The zeta potential of RSNs reached -56 mV with citrate capping, which results in better colloidal stability with the help of electrostatic interactions. These citrate-capped RSNs with a negative surface charge were easily dispersed in a polydimethylsiloxane (PDMS) elastomer matrix and cross-linked to form stretchable magneto-dielectric composites.

Conclusion. Stretchable magneto-dielectric composites were prepared using collectively assembled iron oxide nanostructures as fillers in an elastomer (polydimethylsiloxane) matrix. These raspberry-shaped nanostructures (RSNs), synthesized by a one-pot polyol solvothermal method, consist of oriented aggregates of iron oxide nanocrystals (nanocrystals with common crystallographic orientations directly combined together to form larger ones), which ensure a very low oxidation state of $\text{Fe}_{3-x}\text{O}_4$ nanocrystals and lead to interesting magnetic properties. The oriented aggregation of nanocrystals generates a large interface between nanograins significantly reducing their surface oxidation, improving crystal quality and preventing the formation of surface and volume spin canting. Therefore these iron oxide RSNs display low coercivity with enhanced saturation magnetization (M_s). The use of such citrated RSN as filler material with improved magnetization and low coercivity allowed the fabrication of magneto-dielectric composites that can combine permeability values reaching 2.3 with magnetic loss values limited to 0.11. The resulting composites can also be stretched up to 165% strain before failure due to good adhesion between the elastomer and citrate capped RSNs. In addition, the composition of these fillers was altered to adjust the resonance frequency of the resulting composite material. Stretchable magneto-dielectric composites consisting of maghemite-rich RSNs and magnetite-rich RSNs demonstrated resonance frequencies similar to the spherical ferrimagnetic/ferromagnetic resonance of maghemite and magnetite, respectively.

Conclusions and Future Work

We have demonstrated that raspberry shaped magnetite nanostructures are very interesting and even key elements to fabricate flexible materials with low dielectric loss, high permittivity and permeability values at radio frequencies (1 MHz- 1 GHz). The permeability values achieved by composites made from collectively assembled corona magnetite nanoparticles are significantly higher than the existing magnetite-polymer composites and magnetite-PDMS composites. Additionally, the composites prepared with collectively assembled corona magnetite nanoparticles exhibit an extraordinary magnetic resonance, which changes with the particle size of magnetite nanoparticles. In contrast to these interesting and promising properties of the composites, the composites have high dielectric loss, which can be addressed easily by introducing an insulating layer around the magnetite nanoparticles. We believe such composites could be utilized for high-bandwidth radio frequency antennas as the dielectric loss values are further decreased.

We are currently aiming to identify the origin of the magnetic resonance by characterizing the material in a broader spectrum. Currently synthesis is performed to modulate the nanograin size or to dope the nanostructures with cobalt or manganese or nickel or zinc to modulate the magnetic properties. First experiments with cobalt showed that although similar saturation magnetizations have been obtained, the coercivity is larger as shown in the figure below. Other approaches would be to coat them with carbonaceous materials or silica or gold in collaboration with Dr Yuanzhe Piao.

Remarks : Prof Peter Kofinas has performed courses at Strasbourg (12h eq TD) as invited professor since 2014. Dr Yuanzhe Piao, Pr. Peter Kofinas and Pr S. Begin will co-organize together a symposium to the EMRS spring meeting 2017 entitled : Novel multifunctional nanomaterials for energy, sensing, electronic, and detection technologies.

